Nuclear Inst. and Methods in Physics Research B 475 (2020) 84–88

Contents lists available at ScienceDirect

Nuclear Inst. and Methods in Physics Research B

journal homepage: www.elsevier.com/locate/nimb

# Effective fitting of nanohardness data in two different ferritic steels irradiated with He ions

Yitao Yang[a,b,*], Baoshui Ma[a], Chonghong Zhang[a,b], Xuxiao Han[a,b], Mengke Niu[a,b], Yuguang Chen[a,b], Yin Song[a,b], Zhaonan Ding[a,b]

[a] Institute of Modern Physics, Chinese Academy of Sciences, Lanzhou 730000, China
[b] School of Nuclear Science and Technology, University of Chinese Academy of Sciences, Beijing 100049, China

ARTICLE INFO

*Keywords:*
Irradiation hardening
Nanoindentation
Indentation size effect
Geometrically necessary dislocation

ABSTRACT

A damage plateau (4000 appm/0.25 dpa) was produced in T92 and MA956 by multi-energy He ion irradiation. Nanoindentation was used to characterize the irradiation hardening effect. For the pristine samples, the hardness at the region shallower than 200 nm deviated evidently from the relation predicted by the Nix-Gao model. The hardness of the damaged layer produced by ion irradiation also located in this region. Therefore, a modified model by introducing a maximum allowable density of GNDs proposed by Ruiz-Moreno was used to analyze the hardness data. The fitted result indicated that the hardness of the damaged layer was overestimated by 28.5% for T92 and 48.4% for MA956 in contrast to that obtained from the Nix-Gao model, and a hardening fraction of 64.5% for MA956 and 103.6% for T92 was also obtained. A lower hardening fraction of MA956 was considered to be related to the existence of oxide particles in the matrix.

## 1. Introduction

Structural materials in the fission or fusion reactor are constantly bombarded by neutrons, which results in the cascade damage directly and He production via (n,α)-reaction in materials. The existence of defects formed from cascade damage usually serves as effective sinks capturing neighboring He atoms, which accelerates the aggregation and growth of He/vacancy clusters [1]. This can decrease the ductility and fatigue life, can deteriorate the creep and stress rupture properties and can promote irradiation swelling [2]. All these effects could lead to a drastic deterioration of the mechanical properties of the components [3]. Therefore, the study of irradiation damage in structural materials is of both fundamental and technological interests.

Due to high cost, long time and radioactivity of materials neutron-irradiated in a reactor, ion irradiation is usually used to study the irradiation damage effect in structure materials for its versatility of control on concentration and depth distribution of impurities and damage [4]. However, the projected range of ions is limited to the scale of micrometers, small scale testing technique is needed to measure mechanical properties [5,6]. Nano-indentation is one of the small scale testing techniques and has been widely used to characterize the hardness change in a thin damage layer produced by ion irradiation, e.g. F82H and Inconel 718 irradiated with Fe and He ions [7,8], SS304, Eurofer 97 and Fe-9Cr model alloys irradiated with Fe ions [9], HT-9 irradiated with protons and He ions [10], Eurofer 97 irradiated with He ions [11] and nitride coatings on the multielement high entropy alloy irradiated with N and Au ions [12–14] have been extensively investigated by nanoindentation.

In this study, nanoindentation was used to investigate the materials hardening behavior induced by He in an ODS steel MA956 and a 9Cr F/M steel T92, which are both considered as candidate materials for the structural materials for Generation IV fission reactor and fusion DEMO reactor [15–17]. To avoid the gradient damage effect, He ions with various energies were used to produce a damage/concentration plateau in this study.

## 2. Experiments

The materials used in this study were commercial ODS steel MA956 (Fe-19.4Cr-4.8Al-0.38Ti-0.1Mn-0.51$Y_2O_3$) and 9Cr F/M steel T92 (Fe-8.91Cr-1.67W-0.47Mo-0.43Mn-0.18Si-0.12Ni) obtained from SMC (Special Metals Wiggin Co. Ltd.). The MA956 steel was hot extruded and annealed at 1330°C, the T92 steel was hot rolled, normalized at 1060°C and tempered at 780°C by the manufacturer. Our previous TEM results indicated that T92 samples contained abundant martensitic laths and carbides ($M_{23}C_6$), and the density of dislocations in the martensitic

* Corresponding author at: No. 509 Nanchang Road, Lanzhou 730000, China.
*E-mail address:* yangyt@impcas.ac.cn (Y. Yang).

https://doi.org/10.1016/j.nimb.2020.05.013
Received 9 March 2020; Received in revised form 11 May 2020; Accepted 11 May 2020
Available online 18 May 2020
0168-583X/ 

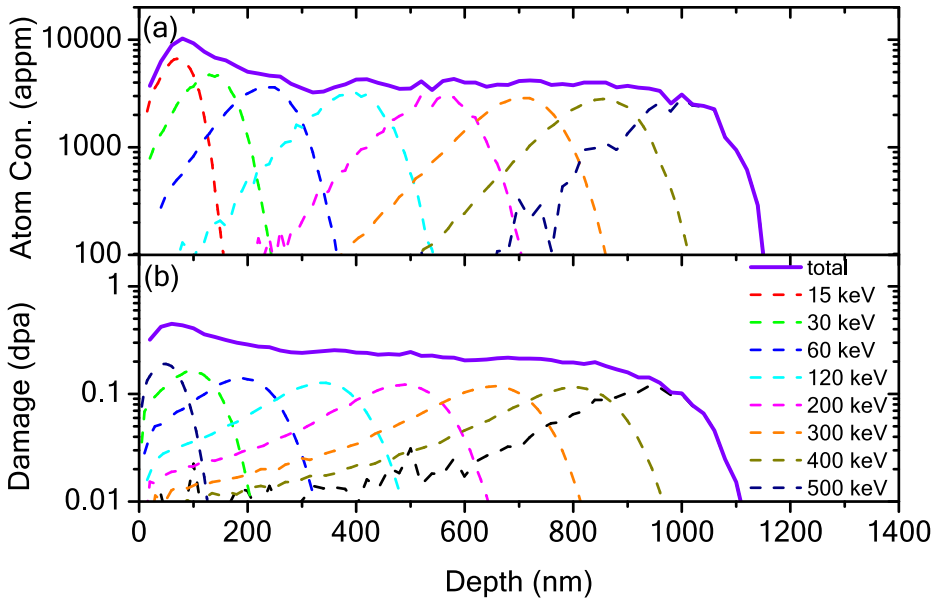


**Fig. 1.** The depth distribution of (a) atom concentration and (b) damage.

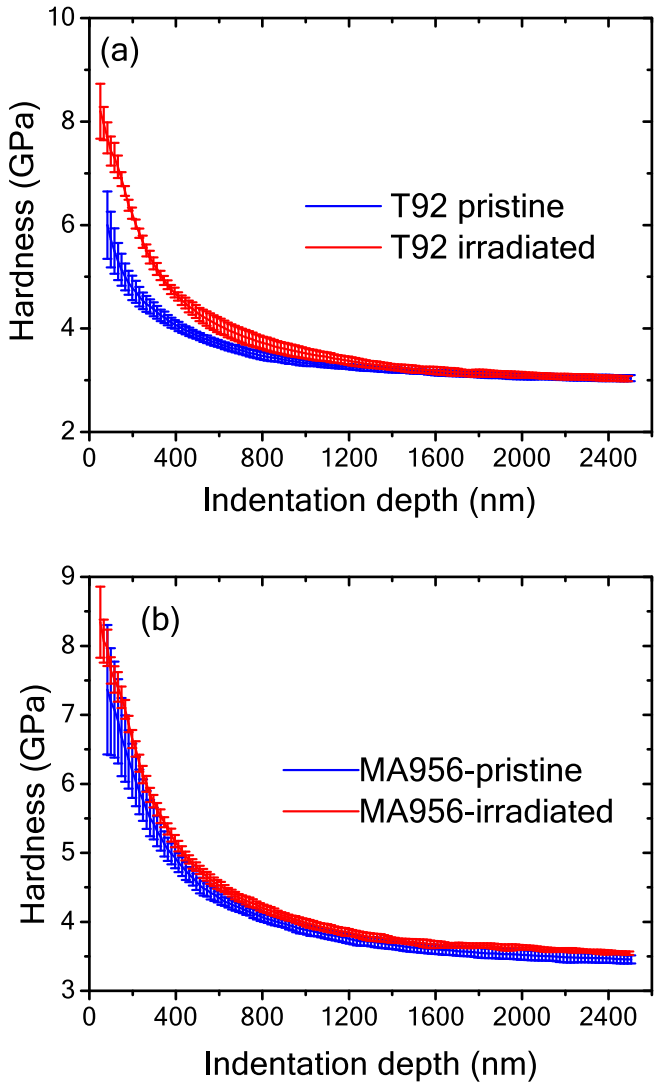


**Fig. 2.** The depth-dependent hardness for the pristine and irradiated T92 (a) and MA956 (b).

laths was extremely high. MA956 samples contained oxide particles with an average size of around 20 nm, the density of the oxide particles reached 8 × $10^{14}$cm$^{-3}$ [18]. Before irradiation, samples with a thickness of 0.5 mm were mechanically ground with SiC abrasive papers (#800-2400) and diamond suspension (diameter ~3 μm), then were electropolished in a mixture solution of 5% perchloric acid and 95% ethanol with the voltage of 30 V for 20 s to remove the stress layer produced by mechanical polishing.

He ion irradiation was performed at room temperature at an irradiation terminal of 320 kV high-voltage platform in the Institute of Modern Physics (IMP), Chinese academy of sciences (CAS). Samples were mounted on a copper sample holder with silver paste to ensure good thermal conductivity. The ion beam was scanned (the frequency ~1.7 kHz) on a 2 × 2 cm$^2$ area for uniform irradiation. To produce a plateau region, He ions with 8 different kinetic energy (15, 30, 60, 120, 200, 300, 400 and 500 keV) were used during irradiation. The ion fluence was 5 × $10^{15}$ ions/cm$^2$ for each irradiation with various energy. The irradiation experiment started with He ions with the highest energy and ended with He ions with the lowest energy. Ion beam intensity sustained at around 10 μA. The distribution of atom concentration and damage with depth obtained from the SRIM 2013 simulation (Kinchin–Pease model, quick calculation, $Ed_{Fe/Cr}$ = 40 eV) are shown in Fig. 1 [19]. It is seen that the atom concentration/damage sustains at 4000 appm/0.25 dpa, the thickness of the damage plateau is 1.1 μm.

Nanoindentation (Nano Indenter G200, Agilent Corp.) was performed to investigate the hardening behavior of materials under irradiation. A diamond Berkovich tip was used with the continuous stiffness measurement (CSM) method (strain rate ~0.05 s$^{-1}$, frequency ~45 Hz, harmonic displacement ~2.0 nm), and the maximum of penetration depth was 2.0 μm. The tip geometry was calibrated from an indentation on fused silica with the same indentation depth. Every sample was subjected to 5 indents with a space larger than 50 μm, the hardness was presented as an average value of the hardness obtained from the 5 independent tests.

## 3. Results and discussions

Fig. 2 shows the results of hardness with depth for the pristine and irradiated samples. To exclude uncertainty factors from the surface, it ignored the data in the region shallower than 50 nm. It is seen that the

hardness increases rapidly with the decrease of indentation depth. This effect is the indentation size effect (ISE), which becomes particularly pronounced in nanoindentation [5,6]. The hardness of irradiated samples in the near-surface region is higher than that of corresponding pristine samples. This indicates that hardening has occurred after He ion irradiation. Compared to T92, MA956 exhibits an inapparent increase of hardness after irradiation in the near-surface region, which indicates that MA956 has better property in hardening resistance during irradiation.

In essentials, for a given material the hardness that describes the material property of resistance to local plastic deformation should be independent of indentation depth. Nix and Gao discussed a model describing ISE based on geometrically necessary dislocation (GND), in which the hardness depth profile is given by the following equation [20],

$$\frac{H}{H_0} = \sqrt{1 + \frac{h_0}{h}}$$

where $H$ is the hardness, $h$ is the indentation depth, $H_0$ is the hardness limit when the indentation depth becomes indefinitely large and $h_0$ is a characteristic length associated with statistically stored dislocation (SSD) density in samples. If $H^2$ is plotted as a function of $1/h$, a linear relation can be found between $H^2$ and $1/h$. This model has been widely used to analyze the hardness data obtained from micro/nano-indentation. Fig. 3 shows the plot of $(H/H_0)^2$ versus $h_0/h$ for the pristine samples. It is seen that a good linear relation can be found between $(H/H_0)^2$ and $h_0/h$ except for the data at the depth shallower than 200 nm, which apparently deviates from the linear relation described by the Nix-Gao model. This phenomenon has been observed for both pristine samples. During sample preparation, the sample was electro-polished after mechanical polishing, and an optical microscope was used to check whether a smooth surface was obtained. Therefore, the hardness deviating from the linear relation caused by artificial factors can be excluded. Furthermore, this deviation has also been found in earlier studies, e.g., in annealed Cu [21] and Ir [22], MgO [23], α-brass and high-purity Al (annealed and work-hardened) [24,25].

For the irradiated samples, the relation of $H^2$ versus $1/h$ is plotted in Fig. 4. An evident deviation of hardness can be observed at the depth deeper than 150 nm for the irradiated samples. From Fig. 1, it is seen that He ion irradiation produces a damage plateau with a thickness of 1.1 μm approximately. During the indentation, the plastic zone beneath the indenter extends gradually from the damage region to the undamaged region with increasing the indentation depth, the corresponding hardness of the undamaged region deviates from the hardness of damaged region. The previous study has indicated that the maximum depth of the plastic zone is about 3–7 times the indentation depth in materials [26,27]. Fig. 4 shows that the turning point locates at the depth of 150 nm approximately, which is consistent with the expected depth of turning point depth (140–160 nm). Earlier studies usually use the Nix-Gao model to directly fit the hardness of the thin damaged region [28]. However, as shown in Fig. 3, the hardness shallower than 200 nm deviates evidently from that predicted by the Nix-Gao model. In other words, the Nix-Gao model overestimates the hardness in the shallower region. Unfortunately, the hardness from the damaged region produced by He ion irradiation in this study also locates in this region (shallower than 150 nm, as shown in Fig. 4). Therefore, it is inappropriate to directly fit the hardness of the damaged region by the Nix-Gao model.

To understand the deviation phenomenon of hardness in the shallower region, earlier studies have considered the influences from indenter tip, surface roughness and intrinsic lattice resistance [29–31]. However, it seems that the effective method to describe the deviation of hardness in the shallower region is introducing a maximum of geometrically necessary dislocations (GNDs) allowed, which is proposed by Huang [29]. The Nix-Gao model assumes that all GNDs are contained in a hemisphere of radius $a$, which equals to the contact radius between indenter and material. This implies that the GNDs distribute uniformly in the storage volume. However, in the case of $a \to 0$, the storage volume tends to zero, while the GND density diverges. The introduction of a maximum of GND allowed tries to solve the divergence of GND density at extremely shallow indentation. Huang uses the spherical coordinates to describe the ISE of indentation, which assumes that GNDs distribute uniformly within a spherical shell of radius $r$ and thickness $dr$ [29]. However, this assumption is not consistent with that GNDs are considered to be contained within cylindrical shells in the Nix-Gao model. Considering the two issues, Ruiz-Moreno et al. give a more generalized form to describe the ISE of hardness obtained from nanoindentation. The hardness is described by the flowing formula [32],

$$H(z) = \frac{1}{2}H_0\left[(2+z)\sqrt{1+z} - \frac{z^2}{2}\ln\frac{2\sqrt{1+z}+2+z}{z\left(1+2\sqrt{\rho_{SSD}/\rho_{GND,\max}+\left(\rho_{SSD}/\rho_{GND,\max}\right)^2}+2\rho_{SSD}/\rho_{GND,\max}\right)} - z^2\sqrt{\rho_{SSD}/\rho_{GND,\max}+\left(\rho_{SSD}/\rho_{GND,\max}\right)^2}\right]$$

where $\rho_{SSD}$ is the density of SSD, $\rho_{GND,max}$ is the maximum density of GND allowed. Parameter $z$ is defined as $h_0/h$, the characteristic depth parameter $h_0 = tan^2\theta/b\rho_{SSD}$, $h$ is the indentation depth. By fitting the hardness data from nanoindentation test, the parameters of $H_0$, $h_0$ and the ratio of $\rho_{SSD}/\rho_{GND,max}$ can be obtained. If Tabor relation and von Mises rule are considered, a strength factor $\alpha$ can also be determined by the relation of $H_0 = 3\sqrt{3}\,\alpha\mu b\sqrt{\rho_{SSD}}$ (Tabor factor is taken as 3.0, $b$ is the Burgers vector, $\mu$ is shear modulus) [32], which is the characteristic of the dislocation interactions governing the flow stress.

The fitted results are shown in Figs. 3 and 5. In Fig. 3, the dashed red line represents the fitted results from the model proposed by Ruiz-Moreno et al. and the dashed water blue line represents the fitted results from the Nix-Gao model. In contrast to the Nix-Gao model, the introduction of maximum allowable GNDs can fit well the deviation of hardness in the shallower region. The irradiated materials contain the damaged and un-damaged layers. Therefore, the hardness data have to be divided into two layers, and the turning point is at around the depth of 150 nm. The corresponding curves fitted by the model proposed by Ruiz- Moreno et al. are shown in Fig. 5. The dashed red line represents the damaged layer and the dashed water blue line represents the substrate layer. The parameters obtained from the fitting for the pristine and irradiated samples are summarized in Table 1.

For the pristine sample, the depth independent hardness obtained from the Nix-Gao model and the model proposed by Ruiz- Moreno is the same. However, for the irradiated samples, the hardness obtained from the Nix-Gao model is higher than that obtained by the model proposed by Ruiz-Moreno. The irradiation hardening effect is overestimated by 28.5% for T92 and 48.4% for MA956. The determined density of SSD and GND is very high. Ruiz-Moreno suggests that the high density of SSD and GND is associated with the martensitic lath structures contained in F/M steels [32]. The strength factor $\alpha$ is determined to be 0.58 and 0.51 for the pristine and irradiated T92 samples, respectively. The martensitic lath in T92 contains a high density of dislocations (lines and loops), the main defects contributed from ion irradiation are dislocation

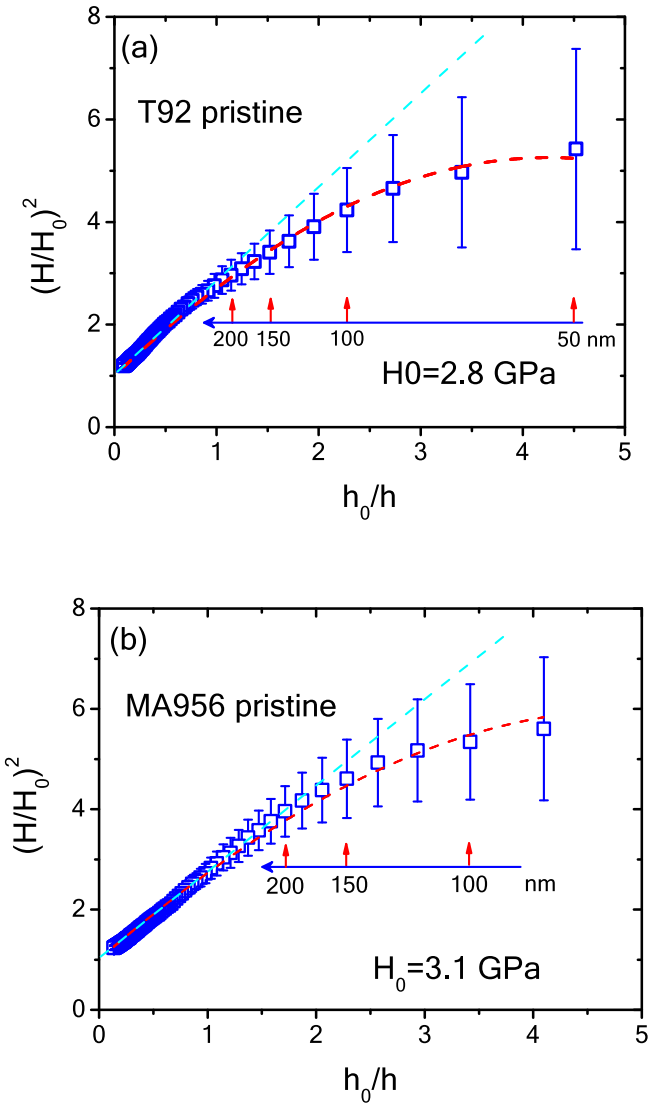


**Fig. 3.** The plot of $(H/H_0)^2$ versus $h_0/h$ for the pristine T92 and MA956.

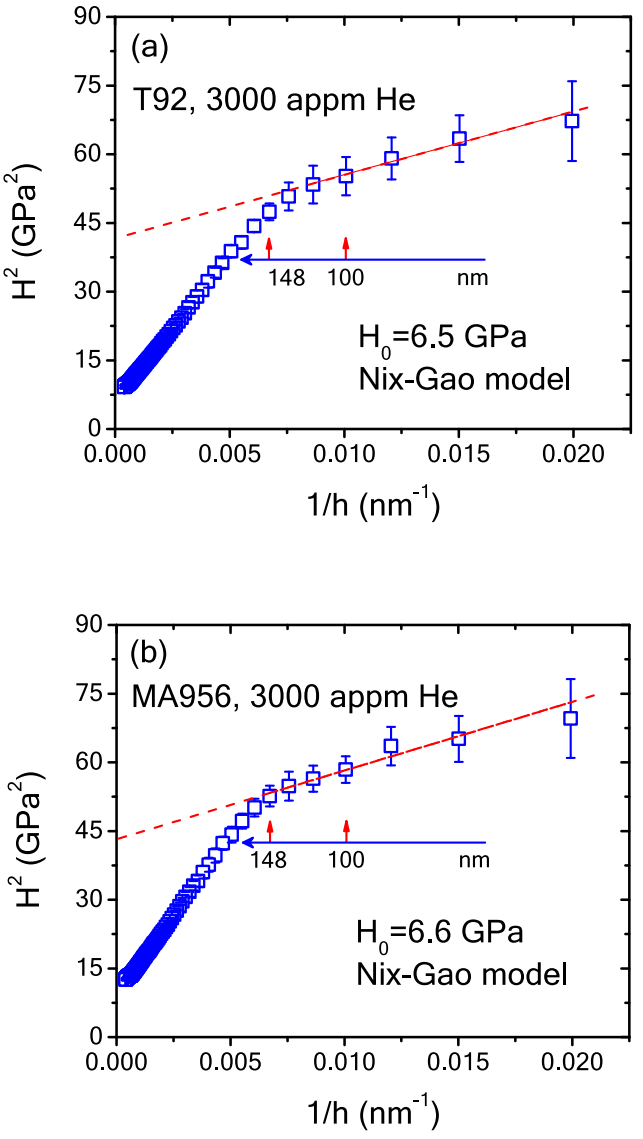


**Fig. 4.** The hardness fitted by Nix-Gao model.

loops. Therefore, the strength factor $\alpha$ for T92 mainly represents the interaction from dislocations (lines and loops), which is consistent with previously reported values for dislocation loops [33]. The strength factor α for MA956 is at around 0.7 (0.77 for the pristine sample and 0.65 for the irradiated sample). MA956 contains a large number of oxides in the matrix, which acts as strengthened phases to improve the strength of materials. Therefore, the interaction of defects in MA956 is different from T92 during indentation, which is considered mainly to be the interaction between oxides and dislocations. Therefore, a higher α value for MA956 is reasonable, which is comparable to the strength factor of precipitates in materials [33].

From the estimated hardness, it is seen that significant irradiation hardening has occurred in T92 and MA956 (103.6% for T92 and 64.5% for MA956). Compared to T92, MA956 demonstrates better irradiation hardening resistance property, which can be attributed to the larger number of oxides dispersed in the matrix. The interfaces between oxides and matrix act as strong sinks for the annihilation of defects produced by ion irradiation, and prevent the further growth of defect clusters. Compared to heavy ion irradiation, He ion irradiation produces significant hardening at similar experiment conditions, e.g. the hardening fraction is only 21% for T92 irradiated to 0.25 dpa with Fe ions at RT [34], but it reaches 103.6% for T92 irradiated to 0.25 dpa with He ions. Previous studies indicate that the introduction of He causes significant coarsening of dislocation loops, e.g. in pure Fe, the size of dislocation loops was 40 nm at 0.8 dpa (Fe ion irradiation), but the size of dislocation loops reached 85 nm in diameter with the existence of He atoms (670 appm He/dpa, Fe + He dual irradiation) [35]. The probable reason for the coarsening of dislocation loops is the occupation of vacancies by He atoms, which prevents the recombination of Frenkel pairs, and further influences on the nucleation and growth of dislocation loops.

## 4. Conclusions

A 9Cr F/M steel T92 and an ODS steel MA956 were irradiated by multi-energy He ions to form a damage plateau at RT. Nanoindentation was used to characterize the hardening induced by He ion irradiation. It was shown that the hardness of the pristine sample at the depth shallower than 200 nm deviated evidently from the linear relation predicted by the Nix-Gao model. Therefore, a modified model proposed by Ruiz-Moreno was used to analyze the hardness data. The fitted result

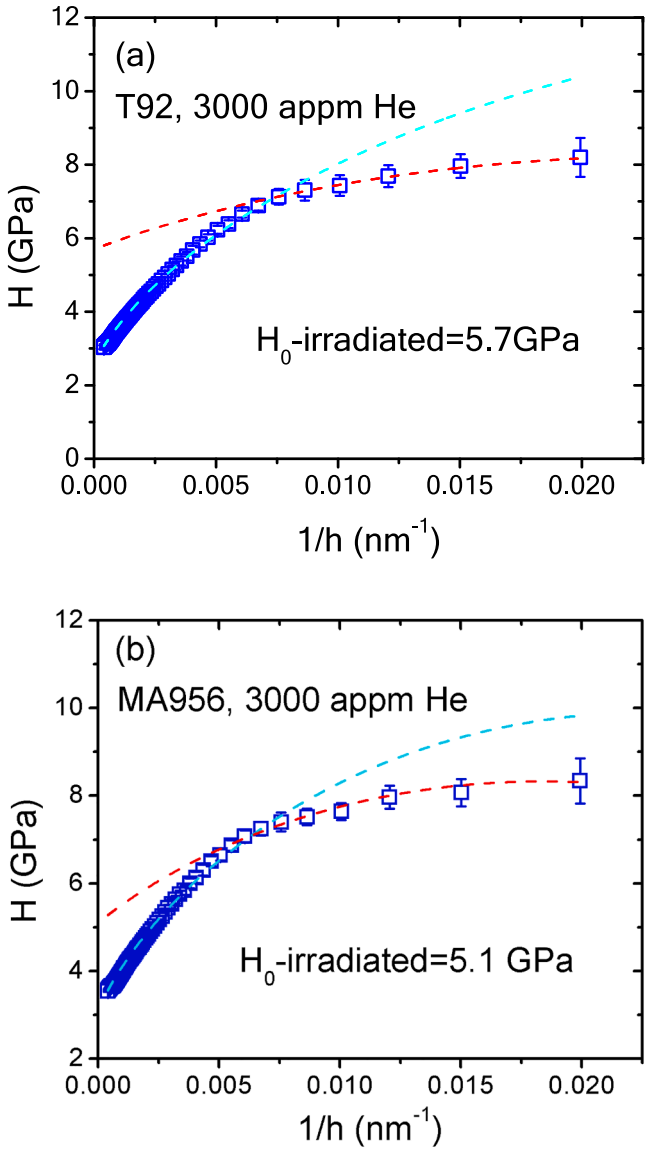


**Fig. 5.** The hardness fitted by the model proposed by Ruiz-Moreno.

**Table 1**
The parameters obtained from the fitting of the model proposed by Ruiz-Moreno. The hardness obtained from Nix-Gao model is also shown in the parentheses for the irradiated samples.

| | T92 | | MA956 | |
|---|---|---|---|---|
| | Pristine | irradiated | Pristine | irradiated |
| $H_0$ (GPa) | 2.8 | 5.7 (6.5) | 3.1 | 5.1 (6.6) |
| $h_0$ (nm) | 235 | 45 | 340 | 90.5 |
| $\rho_{SSD}(\times 10^{15}\ m^{-2})$ | 2.2 | 11.4 | 1.5 | 5.7 |
| $\rho_{GND,max}(\times 10^{15}\ m^{-2})$ | 9.1 | 12.4 | 7.5 | 9.4 |
| $\alpha$ | 0.58 | 0.51 | 0.77 | 0.65 |

indicated that the hardness of the damaged layer was overestimated by 28.5% for T92 and 48.4% for MA956 in contrast to the hardness obtained from the Nix-Gao model. Compared to T92, a lower hardening fraction was obtained for MA 956 (64.5% for MA956 and 103.6% for T92), which suggested that MA956 had better property in hardening resistance. A lower hardening fraction of MA956 was considered as the existence of oxide particles in the matrix.

## CRediT authorship contribution statement

**Yitao Yang:** Methodology, Investigation, Writing - original draft. **Baoshui Ma:** Investigation, Methodology. **Chonghong Zhang:** Supervision, Conceptualization, Writing - review & editing, Formal analysis. **Xuxiao Han:** Investigation, Resources. **Mengke Niu:** Investigation, Resources. **Yuguang Chen:** Investigation. **Yin Song:** Investigation. **Zhaonan Ding:** Investigation.

## Declaration of Competing Interest

The authors declare that they have no known competing financial interests or personal relationships that could have appeared to influence the work reported in this paper.

## Acknowledgments

This study is sponsored by the National Key Research and Development Program of China (Grant No. 2017YFB0702202) and the National Science Foundation of China (Grant No. U1532262, 11475230).

## References

[1] J.D. Hunn, E.H. Lee, T.S. Byun, L.K. Mansur, J. Nucl. Mater. 282 (2000) 131–136.
[2] M. Samaras, Mater. Today 12 (2009) 46–53.
[3] M.A. Pouchon, J. Chen, M. Dobeli, W. Hoffelner, J. Nucl. Mater. 352 (2006) 57–61.
[4] G.S. Was, J. Mater. Res. 30 (2015) 1158.
[5] D. Kiener, A.M. Minor, O. Anderoglu, Y. Wang, S.A. Maloy, P. Hosemann, J. Mater. Res. 27 (21) (2012) 2724.
[6] P. Hosemann, D. Kiener, Y. Wang, S.A. Maloy, J. Nucl. Mater. 425 (2012) 136.
[7] Y. Takayama, R. Kasada, Y. Sakamoto, K. Yabuuchi, A. Kimura, M. Ando, D. Hamaguchi, H. Tanigawa, J. Nucl. Mater. 442 (2013) s23–s27.
[8] J.D. Hunn, E.H. Lee, T.S. Byun, L.K. Mansur, J. Nucl. Mater. 296 (2001) 203–209.
[9] C. Heintze, C. Recknagel, F. Bergner, M. Hernandez-Mayoral, A. Kolitsch, Nucl. Instr. Meth. Phys. Res. B 267 (2009) 1505–1508.
[10] P. Hosemann, C. Vieh, R.R. Greco, S. Kabra, J.A. Valdez, M.J. Cappiello, S.A. Maloy, J. Nucl. Mater. 389 (2009) 239–247.
[11] M. Roldan, P. Fernandez, J. Rams, D. Jimenez-Rey, C.J. Ortiz, R. Vila, J. Nucl. Mater. 448 (2014) 301–309.
[12] A.D. Pogrebnjak, O.V. Bondar, S.O. Borba, G. Abadias, P. Konarski, S.V. Plotnikov, V.M. Beresnev, L.G. Kassenova, P. Drodziel, Nucl. Instr. Meth. Phys. Res. B 385 (2016) 74–83.
[13] A.D. Pogrebnjak, I.V. Yakushchenko, O.V. Bondar, O.V. Sobol, V.M. Beresnev, K. Oyoshi, H. Amekura, Y. Takeda, Phys. Solid State 57 (2015) 1559–1564.
[14] A.D. Pogrebnjak, I.V. Yakushchenko, O.V. Sobol, V.M. Beresnev, A.I. Kupchishin, O.V. Bondar, M.A. Lisovenko, H. Amekura, K. Kono, K. Oyoshi, Y. Takeda, Tech. Phys. 60 (2015) 1176–1183.
[15] Z. Jiao, N. Ham, G.S. Was, J. Nucl. Mater. 367–370 (2007) 440–445.
[16] R.L. Klueh, J.P. Shingledecker, R.W. Swindeman, D.T. Hoelzer, J. Nucl. Mater. 341 (2005) 103–114.
[17] C.H. Zhang, J.S. Jang, M.C. Kim, H.D. Cho, Y.T. Yang, Y.M. Sun, J. Nucl. Mater. 375 (2008) 185–191.
[18] C.H. Zhang, J. Jang, H.D. Cho, Y.T. Yang, J. Nucl. Mater. 386–388 (2009) 457–461.
[19] J.F. Ziegler, J.P. Biersack, U. Littmark, The Stopping and Range of Ions in Solids vol. 1, Pergamon, New York, 1984.
[20] W.D. Nix, H. Gao, J. Mech. Phys. Solids 46 (1998) 411–425.
[21] Y.Y. Lim, M.M. Chaudhri, Philos. Mag. A 79 (12) (1999) 2979–3000.
[22] J.G. Swadener, E.P. George, G.M. Pharr, J. Mech. Phys. Solids 50 (4) (2002) 681–694.
[23] G. Feng, W.D. Nix, Scripta Mater. 51 (6) (2004) 599–603.
[24] A.A. Elmustafa, A.A. Ananda, W.M. Elmahboub, J. Mater. Res. 19 (3) (2004) 768–779.
[25] A.A. Elmustafa, D.S. Stone, J. Mech. Phys. Solids 51 (2) (2003) 357–381.
[26] I. Manika, J. Maniks, J. Phys. D: Appl. Phys. 41 (2008) 074010–074015.
[27] Y. Yang, C. Zhang, Y. Meng, J. Liu, J. Gou, Y. Xian, Y. Song, J. Nucl. Mater. 459 (2015) 1–4.
[28] R. Kasada, Y. Takayama, K. Yabuuchi, A. Kimura, Fusion Eng. Des. 86 (2011) 2658–2661.
[29] Y. Huang, F. Zhang, K.C. Hwang, W.D. Nix, G.M. Pharr, G. Feng, J. Mech. Phys. Solids 54 (8) (2006) 1668–1686.
[30] Y. Liu, A.H.W. Ngan, Scripta Mater. 44 (2) (2001) 237–241.
[31] X. Qiu, Y. Huang, W.D. Nix, Acta Mater. 49 (19) (2001) 3949–3958.
[32] A. Ruiz-Moreno, P. Hahner, Mater. Des. 145 (2018) 168–180.
[33] G.S. Was, Fundamentals of Radiation Materials Science (Metals and Alloys), Springer, 2007.
[34] D. Zhao, S. Li, Y. Wang, F. Liu, X. Wang, J. Nucl. Mater. 511 (2018) 191–199.
[35] D. Brimbal, B. Decamps, J. Henry, E. Meslin, A. Barbu, Acta Mater. 64 (2014) 391.